Open Access Online Journal on Astronomy and Astrophysics

Acta Astrophysica Taurica

www.astrophysicatauricum.org

Acta Astrophys. Tau. 1(1) 1–5 (2020)

doi:10.31059/aat.vol1.iss1.pp1-5

Magnetic power spectrum in undisturbed solar photosphere

V.I. Abramenko, O.K. Kutsenko

Crimean Astrophysical Observatory, Nauchny 298409, Crimea
e-mail: vabramenko@gmail.com

Submitted on November 13, 2019

ABSTRACT

Using the magnetic field data obtained with the Helioseismic and Magnetic Imager (HMI) on board Solar Dynamic Observatory (SDO), an investigation of magnetic power spectra in the undisturbed solar photosphere was performed. We found the following. 1) To get a reliable estimate of a magnetic power spectrum from uniformly distributed quiet-Sun magnetic flux, a sample pattern of no less than 300 pixels length should be adopted. With smaller patterns, energy on all observable scales might be slightly overestimated. 2) For patterns of different magnetic intensity (e.g., a coronal hole, a quiet sun area, an area of super-granulation) the magnetic power spectra in a range of (2.5–10) Mm exhibit very close spectral indices of about −1. The observed spectrum is more shallow than the Kolmogorov-type −5/3 spectrum and it differs from steep spectra of active regions. Such a shallow spectrum cannot be explained by the direct Kolmogorov cascade only, but it can imply a small-scale turbulent dynamo action in a wide range of scales: from tens of mega-meters down to, at least, 2.5 Mm. On smaller scales, the HMI/SDO data do not allow us to reliably derive the shape of the spectrum. 3) Data allow us to conclude that a uniform mechanism of small-scale turbulent dynamo is at work all over the solar surface outside active regions.

Key words: Sun: Magnetic fields; Turbulence; Power Spectrum

1 Introduction

The solar atmosphere is considered to be in a state of turbulence with ubiquitous magnetic field. Strong local magnetic fields are concentrated in active regions (ARs) that are the source of flaring activity of the Sun. These magnetic fields were and still are under thorough analysis, see, e.g. a recent review by Toriumi and Wang (2019). At the same time, only about 20 % of solar photosphere are covered by ARs whereas the rest part of the photosphere is assumed to be undisturbed regions where, however, magnetic fields are still presented. These regions are vast areas of open-configuration magnetic fields – coronal holes (CH), areas of intermittent low-lying magnetic field loops – quiet-Sun areas (QS), vast areas of decayed ARs where the supergranulation is pronounced (we will refer to these regions as SG throughout the rest of the paper). In general, these undisturbed areas contribute significantly to the total magnetic flux (see Fig. 2 in Jin et al., 2011). Magnetic fields in these areas are subject to a meridional circulation during a solar cycle (e.g. Wang et al., 1989; Upton, Hathaway, 2014). They are also an object of turbulent magnetic diffusivity that drastically affects the solar dynamo simulations Dikpati et al. (2006). Thus, thorough study of turbulent processes in weak magnetic fields deserves a particular attention.

One of the powerful instrument to explore turbulence is the calculation and analysis of the power spectrum. Developed homogeneous isotropic turbulence is characterized by a Kolmogorov spectrum $E(K) \sim k^{(-\alpha)}$ with the spectral index $\alpha = 5/3$ (Kolmogorov, 1941). Under these conditions the system evolves in a quasi-equilibrium state: energy injection on large scales is compensated by energy dissipation on small scales, a phenomenon known as the direct Kolmogorov cascade when larger structures disintegrate forming smaller ones, and so on until the dissipation scale. A deviation of the spectrum from the Kolmogorov-type spectrum implies disequilibrium (as observed in ARs, e.g. Abramenko, 2005), or the presence of other energy injection mechanisms in the intermediate scales (inside the so-called inertial range between the injection scale and dissipation scale).

Insufficient attention was paid to undisturbed solar areas during previous analyses of solar magnetic power spectra. Thus, magnetic power spectra of ARs were studied in detail (Abramenko, 2005; Abramenko, Yurchyshyn, 2010; Hewett et al., 2008; Katsukawa, Orozco Suarez, 2012) especially after the discovery of the relationship between the spectral index and flare productivity of ARs (Abramenko et al., 2001). In the present study, we intend to fill this gap. Uninterrupted full-disk observations of the Sun carrying out by the Solar Dynamics Observatory (SDO, Schou et al., 2012) allow us to make such an analysis.

2 Data and method

We employed magnetic field data acquired by the Helioseismic and Magnetic Imager (HMI, Schou et al., 2012) instrument on board SDO. Line-of-sight full-disk magnetograms in M-720s mode were obtained with the spatial resolution of 1″

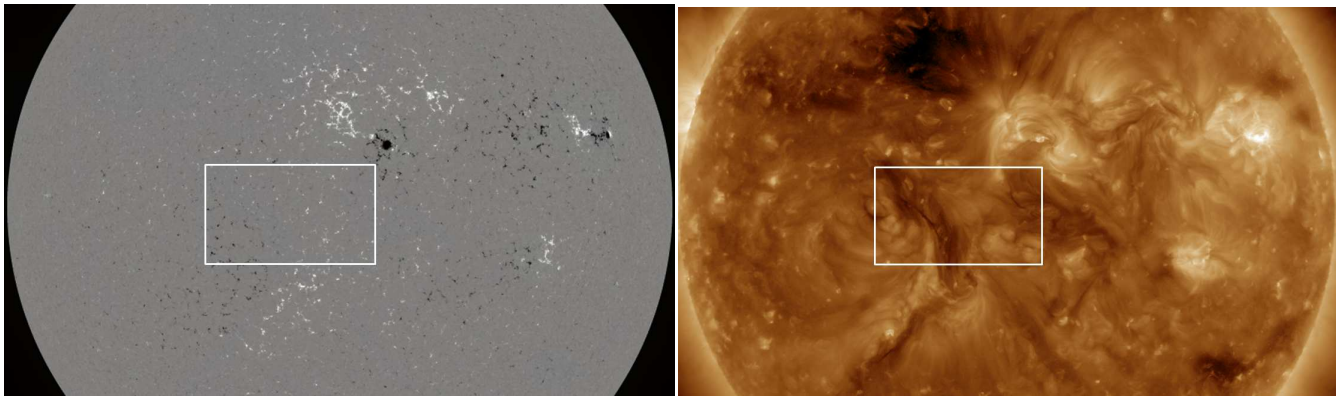

Fig. 1. SDO/HMI magnetogramm (left) and SDO/AIA/193 Å intensity (right) acquired on 2017 June 19 at 19:24 UT. The white rectangle outlines the region under study (930 × 530 pixels), where overlapping boxes of a given size were selected and the magnetic power spectra for each one were calculated (see Table 1)

Table 1. Parameters of the magnetic field for 7 runs with different size of the sample boxes selected inside the white rectangular area in Fig. 1

Size, pixels	$(< B_z^2 >)^{1/2}$, Gs	$F/(10'' \times 10''), 10^{18}$ Mx	α
100×100	21.6 ± 18	3.80 ± 0.9	-0.942 ± 0.077
150×150	20.3 ± 15	3.68 ± 0.6	-0.881 ± 0.080
200×200	19.9 ± 14	3.62 ± 0.5	-0.822 ± 0.067
300×300	18.6 ± 11	3.50 ± 0.3	-0.887 ± 0.060
400×400	18.0 ± 8	3.48 ± 0.2	-0.846 ± 0.040
660×500	18.5 ± 4	3.51 ± 0.03	-0.843 ± 0.031
930×530	19.0	3.53	-0.920

(pixel size 0.5″). Regions under study were located near the solar disc center, so that the projection effect was neglected. We investigated areas in the undisturbed solar photosphere, i.e. outside ARs.

Magnetic power spectra were calculated using the approach described in Abramenko et al. (2001) and Abramenko (2005). First, a two-dimensional Fourier Transform of a magnetogram was calculated. Then, squared Fourier Transform was integrated within a thin annulus between two concentric rings in the two-dimensional space of wavenumbers yielding the one-dimensional power spectrum $E(k)$. Here $k = 2\pi/r$ is the wavenumber and r is the spatial scale in Mm. The choice of the inertial range for calculation of the spectral index α and the influence of instrumental effects on the shape of the spectrum were considered in Abramenko et al. (2001). Abramenko (2016) argued that the inertial range for power spectra derived from SDO/HMI magnetograms should be set between 2.4 and 10 Mm.

3 Influence of the size of sample pattern on power spectrum accuracy

For the power spectrum calculation it is necessary to select some finite rectangular area of the solar surface amidst the vast undisturbed photosphere. Therefore, it is important to find out how the choice of the area size affects the shape of the spectrum and what minimal area size is sufficient for the reliable spectrum calculation. To solve these problems, we chose an area of undisturbed photosphere in the center of the solar disc observed on June 19, 2017 (Fig. 1). As it can be seen in the figure, this area is a region of weak magnetic fields (left panel). From the SDO/AIA/193 Å image of the disc

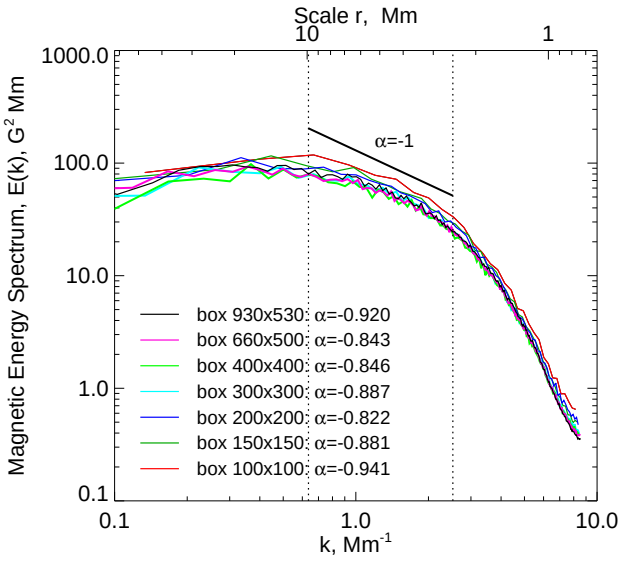

Fig. 2. Power spectra averaged over 25 boxes of the same size. Dotted vertical lines enclose the wavenumber range (2.5–10 Mm) where the power index α was determined by the best-linear fitting of the curve

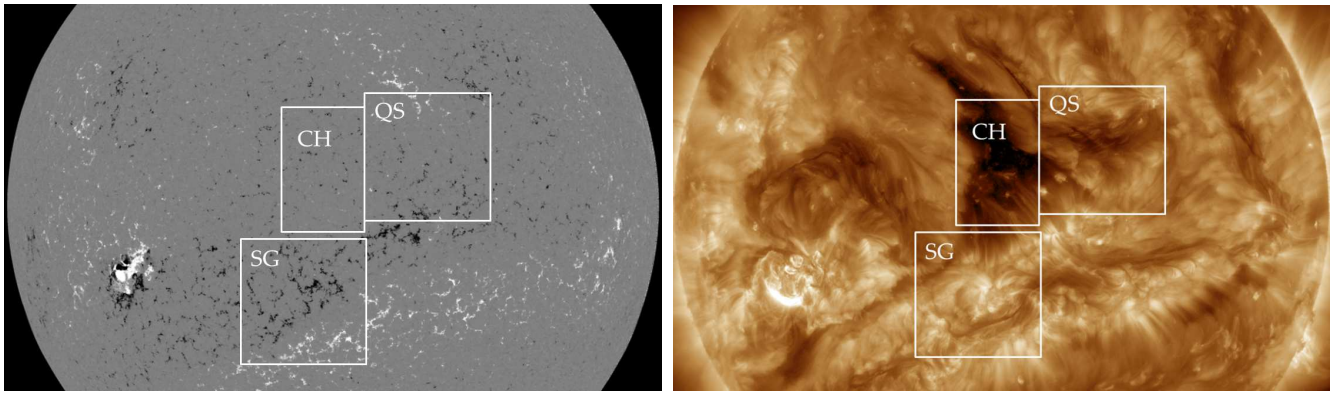

Fig. 3. SDO/HMI magnetogramm (left) and SDO/AIA/193 Å solar disk image acquired on 2015 March 3 at 01:13 UT. Rectangles enclose regions of undisturbed solar photosphere under analysis: CH – coronal hole, QS – quiet Sun, SG – well-pronounced supergranular network field

(right panel) we concluded that the area is a region of closed loops, not a coronal hole. A size of the area under study was 930×530 pixels (465″×265″), or 340×190 Mm (highlighted by a white rectangle in Fig. 1). We selected 25 overlapping boxes of a given size within the selected rectangle. The box size was consequently increased and centers of boxes were shifted within the rectangle. At the first step the boxes with the size of 100×100 pixels were selected, at second stage – 150×150 pixels, and so on until the maximum size was reached. The data on the size of the boxes and magnetic field parameters are presented in Table 1.

Magnetic field and power spectrum parameters averaged over the 25 boxes of a given size are listed in Table 1. The mean-square value of magnetic flux density $(< B_z^2 >)^{1/2}$ is shown in the second column. The values of the unsigned magnetic flux F which was calculated as a sum of absolute values of fluxes in pixels and normalized to the $10'' \times 10''$ area (the unit area) are presented in the third column. Table 1 shows that the flux density and magnetic flux per unit area become enhanced when sub-regions of small sizes (100–200 pixels) are considered. Relative to the data for larger boxes, the flux density is overestimated by 8–17% (and by 11% on average) and the magnetic flux is overestimated by 3–8% (and by 5% on average). We suppose that the observed for smallest sample boxes overestimation of the field parameters is artificial and caused by inhomogeneity of the quiet sun magnetic structure, which becomes noticeable on these rather small scales. Low statistics for small sample boxes also can contribute.

The spectral index α was calculated as the slope of the power spectrum within the (2.5–10) Mm inertial range. Power spectra averaged over the 25 boxes of a given size are shown in different colors in Fig. 2. The spectrum for the smallest box is above the others over all scales. The spectra for boxes of 300×300 pixels and larger are more close to each other, in accordance with the similarity of their field parameters in Table 1. The power index spectrum is $< \alpha > \pm 1.5\sigma = -0.877 \pm 0.064$.

Comparison with spectrum $E(k) \sim k^{-1}$ demonstrates that the slope of -1 is retained even better within a narrower interval, e.g., (2.5–7) Mm. Presumably, in a very weak magnetic field zone (similar to the one considered here) the supergranular network of the magnetic field does not exhibit itself and there is not enough magnetic elements with the sizes of more than 7 Mm, which results in a lack of energy on that scales.

4 Power spectrum in patterns of different magnetic intensity in undisturbed photosphere

To analyze the power spectra in undisturbed photosphere from the weakest magnetic-field zone (coronal hole) to quiet Sun and then to the strongest zone of super-granular network, the data acquired on 2015 March 10 were chosen (Fig. 3). A coronal hole region and a quiet Sun region are labeled as CH and QS, respectively. An area of decayed NOAA active regions 12242–12259, that were presented at this location 3–4 rotations ago, is marked as SG (super-granular network).

To improve the accuracy, we used 11 HMI magnetograms acquired between 00:00 and 02:00 UT with 12 min cadence. The spectral and field parameters were averaged over the 11 magnetograms. Using the method described in previous section, we calculated the mean-squared magnetic flux density $(< B_z^2 >)^{1/2}$, the value of unsigned magnetic flux F, normalized by $10'' \times 10''$ area, and spectral index α. The results are presented in Fig. 4 and Table 2.

Figure 4 shows that all spectra demonstrate a gradual bend on wavenumbers $k \approx 2.5$ Mm^{-1} corresponding to the linear scale $r = 2\pi/k \approx 2.5$ Mm. According to Abramenko et al. (2001), an artificial power decrease in the high-frequency part of the spectrum (i.e. on small scales) manifests itself on scales of approximately 2.5–3 times larger than the telescope resolution limit. For the space-based instrument SDO/HMI, this limit equals to the diffraction limit. SDO/HMI diffraction limit equals to

$$\Theta = 1.22 \cdot 0.0206 \frac{\lambda}{D} = 1.11'' = 0.803 \text{ Mm}. \quad (1)$$

Here $\lambda = 617.3$ – is the wavelength of observations (in nm), $D = 14$ – is the telescope diameter (in cm). The constant 1.22 is derived from the Rayleigh criterion for the diffraction limit of optical system. The triple Θ spatial scale is approximately 2.4 Mm. This is close to the 2.5 Mm value estimated

Table 2. Parameters of the photosphere regions for the observations on 2015 March 3

Region	$(< B_z^2 >)^{1/2}$, Gs	$F/(10'' \times 10''), 10^{18}$ Mx	α
CH	19.5 ± 5	3.74 ± 0.06	-1.116 ± 0.039
QS	33.4 ± 4	5.87 ± 0.04	-1.153 ± 0.023
SG	63.0 ± 8	11.43 ± 0.08	-1.163 ± 0.022

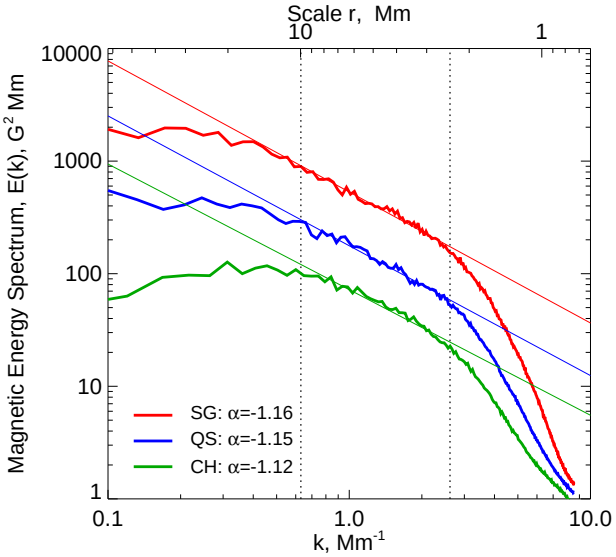

Fig. 4. Magnetic power spectra of three regions of undisturbited solar photosphere depicted in Fig. 3. The lowest spectrum corresponds to coronal hole, CH, middle spectrum –to quiet Sun region, QS, upper spectrum – supergranular network field, SG. Dotted vertical lines enclose the wavenumber range (2.5–10 Mm) where the power index α was determined. The thin lines demonstrate the best–linear fits to the data

from the spectrum. Therefore, observed power decrease on scales $r < 2.5$ Mm is artificial, and is caused by insufficient sensitivity and low resolution of the instrument. The shape of the spectrum on scales exceeding 2.5 Mm seems to be reliable.

As it can be seen in Fig. 4, during the transfer from the weakest to the strongest magnetic environment (e.g., from CH to QS to SG), the spectrum moves up (power increases on all scales) and stretches to the left (e.g., to the larger scales). Presumably, the effects are caused by the contribution of super-granulation network fields to the spectrum. However, the most unexpected and interesting result in our opinion is the permanence of the spectral slope for all zones. The spectrum remains similar to non-Kolmogorov $E(k) \sim k^{-1}$, more precisely, -1.14 ± 0.02.

5 Conclusion

The analysis of magnetic power spectra in undisturbed solar photosphere allowed us to obtain two types of results: methodological and physical ones. Methodological result can be formulated as follows:

– To obtain a reliable estimate of the power spectrum in a wide zone with quasi-uniform distribution of magnetic field the region under study should be no smaller than 300 pixels in length. Using a smaller region yields a slight overestimation of magnetic power on all available scales; the mean-square flux density and normalized unsigned flux can be also overestimated by about 11% and 5%, respectively.

Physical conclusions.

– For different magnetic zones of undisturbed photosphere, namely, for a coronal hole, quiet Sun, and supergranular network field, the magnetic power spectrum exhibits identical spectral index of approximately -1.14 ± 0.02. The spectrum is more shallow than the Kolmogorov $-5/3$ spectrum and it significantly differs from steep spectra of active regions (see, e.g., Abramenko, Yurchyshyn, 2010)
– The k^{-1} spectrum can not be explained only by the direct Kolmogorov cascade with slope $-5/3$. This result might be a consequence of additional generation of magnetic energy due to small-scale turbulent dynamo (Karak, Brandenburg, 2016). Apparently, the generation takes place in a wide range of scales from at least 2.5 Mm to tens of megameters. The spectral shape cannot be estimated correctly at scales less that 2.5 Mm using SDO/HMI data. However, the presence of turbulent dynamo at lower scales cannot be excluded.
– The data allowed us to conclude that the same mechanism of small-scale turbulent dynamo takes place within the whole solar surface outside active regions. This conclusion agrees with Ishikawa and Tsuneta (2009) results. Undoubtedly, the three-dimensional organization of the magnetic field above the photosphere differs in coronal hole and quiet Sun region. Substantial part of flux is concentrated in open fields in CH and in closed low loops in quiet regions (see, e.g., Hofmeister et al., 2019). Our analysis demonstrates that in spite of considerable difference in the 3D-configuration of magnetic loops above the photosphere, the subsurface dynamo processes are quite similar. Apparently, the nature of these processes is the generation of magnetic flux by turbulent medium on a whole spectrum of scales: from minimal in CH to larger in QS and SG.

It should be mentioned that according to the investigation of solar wind at 1 AU distance (Kiyani et al., 2011), the low-frequency range gives the power spectrum slope of -1.00 ± -0.04. This coincides with our result -1.1 for the undisturbed regions. This fact hardly can be a coincidence since in both cases the solar magnetic field attends as common agent.

Acknowledgements. We are grateful to the referee for supporting remarks, an interest to the paper and useful comments.

References

Abramenko V.I., 2005. Astrophys. J., vol. 629, p. 1141.
Abramenko V.I., 2016. Turbulent and multi-fractal nature of solar magnetism (Dr. Sci. thesis). Nauchny. (In Russ.)
Abramenko V.I., Yurchyshyn V.B., 2010. Astrophys. J., vol. 722, p. 122.
Abramenko V., Yurchyshyn V., Wang H., Goode P.R., 2001. Solar Phys., vol. 201, p. 225.
Dikpati M., Gilman P.A., 2006. Astrophys. J., vol. 649, p. 498.
Hewett R.J., Gallagher P.T., McAteer R.T.J., et al., 2008. Solar Phys., vol. 248, p. 311.
Hofmeister S.J., Utz D., Heinemann S.G., Veronig A., Temmer T., 2019. Astron Astrophys., vol. 629, p. 22.
Ishikawa R., Tsuneta S., 2009. Astron Astrophys., vol. 495, p. 607.
Jin C.L., Wang J.X., Zhao H., 2011. Astrophys. J., vol. 731, p. 37.
Karak B.B., Brandenburg A., 2016. Astrophys. J., vol. 816, p. 28.
Katsukawa Y., Orozco Suarez D., 2012. Astrophys. J., vol. 758, p. 139.
Kiyani K.H., Osman K.T., Chapman S.C., 2015. Phil. Trans. R. Soc. A, vol. 373, id. 20140155, doi:10.1098/rsta.2014.0155.
Kolmogorov A.N., 1941. Doklady Akad. nauk, vol. 30, p. 301. (in Russ.)
Schou J., Scherrer P.H., Bush R.I., et al., 2012. Solar Phys., vol. 275, p. 229.
Toriumi S., Wang H., 2019. Living Rev. Sol. Phys., vol. 16, no. 1, p. 3.
Upton L., Hathaway D., 2014. Astrophys. J., vol. 780, p. 5.
Wang Y.-M., Nash A.G., Sheeley N.R., 1989. Jr. Science, vol. 245, no. 4919, pp. 712–718.